Numerical modeling of the solid-state sintering at the microstructural level: Multiphysics approach and application to metal additive manufacturing

Judice Cumbunga, Said Abboudi, Dominique Chamoret, Samuel Gomes

Numerical modeling of the solid-state sintering at the microstructural level: Multiphysics approach and application to metal additive manufacturing

Judice CUMBUNGA[(1,2)], Said ABBOUDI[(1)] , Dominique CHAMORET[(1)] , Samuel GOMES[(1)]
[(1)]ICB-COMM UMR 6303, CNRS, Univ. Bourgogne Franche-Comté, UTBM
[(2)] Department of Mechanics, Faculty of Engineering, Agostinho Neto University
Email: judice.cumbunga@utbm.fr

Abstract - The application of the additive manufacturing process for metals has become increasingly important in industrial manufacturing, mainly due to its ability to process components with complex geometry. Several 3D printing technologies for metals have been studied, such as Bound Metal Deposition (BMD), a process that allows the manufacture of components by applying three steps, design, printing, and sintering. In the case of this technology, the sintering process, as a thermal treatment, is one of the indispensable steps in the additive manufacturing of metals, allowing the properties of the materials obtained by this type of manufacturing technology to be improved. The holistic modeling of the sintering process is still a challenge for researchers because of the complexity in capturing computationally the microstructure evolution during the process and its coupling with other physical phenomena (thermal and mechanical). A multiphysics numerical approach based on a coupling of thermal, mechanical and phase fields is proposed as an alternative to predict the microstructure evolution and thermomechanical properties of 316L stainless steel during the sintering process. In this context, a numerical model based on the finite element method is proposed as an alternative to evaluate the impact of the thermal field, as the activation force of the sintering process, on the microstructure field evolution and, in turn, the impact of the evolution of phase field variables on the thermal and mechanical properties of the studied material. The model is applied for different sintering temperature and time, allowing the influence of these parameters on the microstructure evolution and on the thermomechanical properties of the material to be evaluated.

Keywords: Solid-state sintering, microstructure evolution, multiphysics coupling, metal additive manufacturing, finite element method, stain steel 316L.

I. INTRODUCTION

The manufacture of component or structure with complex geometry and functional as to its application, has been a great challenge for researchers. Additive manufacturing [1]–[3] and sintering [4]–[6], both combined, have increasingly established themselves as promising alternatives to solve this particular problem in cases of metal components or structures. For additive manufacturing technology for metals, known as Bound Metal Deposition (BMD), a Material Extrusion (Mex) technology, the manufacturing process of a component is divided into four steps, design [7]–[9], printing, debinding and sintering [10], [11], [3]. Despite their relative affordability and the ability to produce parts with high geometrical accuracy, these parts suffer from high porosity and poor surface finishes [3]. To overcome these kinds of problems, sintering is usually applied, which is a processing technique for producing density-controlled materials and components from metal or ceramic powders by applying thermal energy [6], [12], i.e. it is a thermal treatment, although in some cases external pressure is also applied [13].

The improvement of existing sintering techniques, by computational modelling and experimental approach, is capital to meet the growing demand for a wide range of technologically significant systems, including, for example, fuel and solar cell components, electronic and computer elements, bioimplants elements, thermoelectric materials, drilling tools in the oil and gas industry, etc.[12]. So the use of sintering techniques for processing metal materials to manufacture additively parts with structural and functional applications will continue to be a challenge for the coming years [12], [14]. Although sintering is relatively well studied for Metal Injection Molding (MIM) processes [6], [15]–[17], research is insufficient or practically non-existent for metal additive manufacturing (MAM), especially in the field of computational modeling, where the main challenges lie in the study of the behavior of material properties after applying this type of heat treatment.

Computational modeling of the sintering process is extremely complex because it is a process characterized as being multi-physical and multi-scale. It is considered to be a multi-physical process because it results from the combination of thermal, mass

diffusion, and mechanical phenomena, and as a multi-scale process because it occurs at the microscopic level, due to the microstructural evolution of the material during the process. These microstructural developments have an impact on the macroscopic behavior, resulting in distortions, shrinkage, porosity reduction, and in the improvement of the surface quality of the component or structure. The macroscopic modeling of the sintering process will always have as its main input the microstructural evolution of the material [18], [19], so it is fundamental to study the sintering process at the microstructural level, to later couple it with the macrostructural effects, in order to obtain the holistic behavior of the process.

The holistic modeling of the sintering process is highly dependent on the techniques applied to capture the microstructure evolution. Various computational models based on different approaches have been developed and/or improved to predict the material behavior [20]–[22]. In the last few decades, the field-phase method (PFM) has been widely applied to study the evolution of microstructure [11], since it has proven to be a very powerful tool to associate the evolution of microstructure with other physical phenomena [13]. Details on the application of PFM coupled with thermal and mechanical to study sintering process at microstructure level was recently introduced by Sudipta et al. [13], the approach was based on first proposal for applying the phase field method to model the sintering process made by Wang [23], and this proposal has given rise to several works in this field, not only limited to the simulation of two particles in 2D but extending to more than two particles and in 3D[12], [13], [22]–[27]. The purpose of this paper is to numerically model the behavior of the sintering process at microstructural level considering a multiphysics approach based on a coupling of thermal, mechanical and phase-field method, to predict the microstructure evolution and thermomechanical properties of 316L stainless steel obtained by Bound Metal Deposition (BMD).

A numerical model based on the finite element method is proposed as an alternative to evaluate the impact of the thermal field on the microstructural field evolution and, in turn, the impact of the evolution of phase field variables on the thermal and mechanical properties of the material. The model is applied for different sintering temperature and time, in order to evaluate the influence of these parameters on the microstructure evolution and on the thermomechanical properties of the material.

II. MULTIPHYSICS MODELING APPROACH AND FORMULATION

A. *Thermal field formulation*

In the pressure-less solid state sintering process, thermal loading plays an important role in activating different diffusion mechanisms during sintering and controlling the morphological changes [23]. To obtain the temporal and spatial variations of the temperature during the process, the Fourier law for transient heat conduction is applied, according to the equation below:

$$\rho(T)c_p(T)\frac{\partial T}{\partial t} = \nabla \cdot (k(T)\nabla T) + \dot{q_g} \qquad (1)$$

This equation is solved by considering that the thermal properties of the material such as thermal conductivity k and specific heat c_p, and density ρ, vary with temperature and microstructure evolutions. On the other hand, it was assumed that is the rate of heat generation $\dot{q_g}$, is caused by reduction of $\dot{F}$, that is rate of total free energy per unity of volume and will be calculated from Phase field sintering model [23], [27], [28], but since this value is very low compared to the amount of energy coming from the sintering environment, its effect on the thermal field can be neglected.

B. *Phase field formulation (Microstructural field)*

The study of the microstructural evolution during the sintering process is very important since it allows to obtain the constitutive behavior of the material. The phase field model (PFM) has been widely applied to model the microstructure evolution. A sets of order parameters are used to describe the microstructure [23], [27], conserved order parameter (c), that distinguish the phases between porous (c = 0) and solid (c = 1), and non-conserved parameter (η), that describe individual grains with different crystal orientations [23], [27]. These parameters are considered as continuum field functions (the so-called phase fields), and describe the sizes, shapes, and spatial arrangement of particles of different compositions, lattice symmetries, and crystallographic orientations, i.e., the microstructure evolution during material processing [23].

The reduction of the total free energy through diffusion mechanisms and structural relaxation drives the microstructure evolution. The total free energy of a material is a function of conserved and non-conserved order parameters, which can be the combination of bulk chemical free energy, interfacial energy, elastic energy, visco-plastic energy, and external energy source, as described in equation 2, but in this study, the system energy, elastic and visco-plastic energy are ignored.

$$F = F_{chem} + F_{int} + F_{el} + F_{vp} + F_{sys} \qquad (2)$$

Two types of continuum equations govern the phase field model for sintering, proposed by Wang [23], who added the rigid-body motion into the Cahn-Hillard equation [29], [30],

used to describe the behavior of conserved phase variables, and into the Allen-Cahn equation [29], used to describe the behavior of non-conserved phase variables.

$$\frac{\partial c}{\partial t} = \nabla \cdot \left(\mathrm{M} \nabla \frac{\delta F}{\delta c} - c \sum v_{adv} \right) \quad (3)$$

$$\frac{\partial \eta_i}{\partial t} = -L \frac{\delta F}{\partial \eta_i} - \nabla \cdot \left[\eta_i v_{adv_i} \right] \quad (4)$$

where M and L are the mobility coefficients associated with the corresponding order parameters c and η, and are temperature dependence, v_{adv} is the advection velocity. F, the system total free energy, is the driven force for the evolution, and its reduction is achieved by the multiple mechanisms of mass transport and structural relaxation (surface diffusion, grain boundary diffusion, volume diffusion, vapor transport, and grain boundary migration).

The kinetics of the microstructural evolution of the sintering process is represented by equations (6) and (7), and their solution predicts the temporal and spatial evolutions of the field variables. For more details about the phase field approach to modeling the sintering process, see [12], [22], [23], [26], [27], [29]–[31].

C. Mechanical field formulation

Activated by the effect of gravity, the mechanical field plays a very important role in the computational modeling of the solid state sintering process, contributing to the reduction of porosity at the microstructural level, improving the density of the component or structure, but also inducing deformations on it. As mentioned in point B of section II, and represented in equation 2, concerning the mechanical field, it was only considered the contribution of the elastic energy on the microstructural evolution, by including this effect on the total energy of the system.

The strain for a linear elastic and isotropic solid during phase transformation is caused by elastic stress, and is computed from the displacements, while the corresponding stresses are computed using Hook's law.

$$\varepsilon_{ij}^{el} = \frac{1}{2}\left[\frac{\partial u_i}{\partial x_j} + \frac{\partial u_j}{\partial x_i}\right] \quad \text{and} \quad \sigma_{kl} = C_{ijkl}(T)\varepsilon_{kl}^{el} \quad (5)$$

The displacement components are obtained by solving the equilibrium equation.

$$\nabla \cdot \sigma_{ij} + b_i = 0 \quad (6)$$

In the Solid-state sintering, the body-force is the gravitational force, and, in current study is ignored and replaced by a load in the top of the body.

The first steps to couple elasticity with PFM was proposed by Kachaturyan [32], then other studies came out using the same approach [29], [33]–[35], and recently it has been applied to sintering [13]. The elastic energy is computed according to equation (7).

$$f_{el} = \frac{1}{2}\int_V C_{ijkl}(\vec{r})\, \varepsilon_{ij}^{el} \varepsilon_{kl}^{el} d\vec{r} \quad (7)$$

Where, $C_{ijkl}(\vec{r})$, are the components of the elastic modulus tensor, that is function of temperature, ε_{ij}^{el} and ε_{kl}^{el} the strains, and i, j, k, l the suffix indices associate with the direction used to identify the components of the stresses and strains.

D. Multiphysics coupling

The holistic modeling of the sintering process is achieved by coupling three physical phenomena (thermal, mechanical, and microstructural fields). This coupling is defined by various relationships among the fields, such as thermo-mechanical, thermo-microstructural, and mechano-microstructural coupling.

1) Thermo-microstructural coupling

The spatial and temporal distribution of temperature leads to the activation of the microstructural field through the mechanisms of mass transport (diffusion process), which are represented by the Cahn-Hilliard (equation 3) and Allen-Cahn mobility (equation 4). On the other hand, microstructural evolution influences the thermal field in two ways, first, it causes an addition of chemical free energy and interfacial energy on the thermal field governing equation, and second, material properties (density, thermal conductivity and, specific heat) become dependent on phase field variables.

In this study, the relationships considered between the two fields were as follows:

- From the thermal field to the microstructure, the temperature distribution is applied to compute the Cahn-Hillard and Allen-Cahn mobility.
- From the microstructural to the thermal field, the influence of the chemical free and interfacial energies on the thermal field was neglected, and only the variation of the thermal properties with respect to the phase field variables was considered, according the equation 8 [13].

$$\mathrm{M} = \mathrm{h(c)M_{particle}} + \big(1 - \mathrm{h(c)}\big)\mathrm{M_{void}}\,, \mathrm{h(c)} = 3\mathrm{c}^2 - 2\mathrm{c}^3 \quad (8)$$

Where $h(c)$, is the interpolation function, $M_{particle}$ and M_{void} are material properties for particles and voids respectively, and considering that material properties for voids are neglected.

The variation of thermal properties (density, thermal conductivity and specific heat) with respect to temperature and conserved parameter, are:

$$\rho(T,c) = \rho(T) \cdot (3c^2 - 2c^3) \quad (9)$$
$$k(T,c) = k(T) \cdot (3c^2 - 2c^3) \quad (10)$$
$$c_p(T,c) = c_p(T) \cdot (3c^2 - 2c^3) \quad (11)$$

2) Mechanical and microstructural coupling

The microstructure evolution occurs in such a way that the material properties become dependent on the phase field variables, while the elastic energy resulting from the mechanical transformations is added to the equations that govern the microstructural field.

Elastic energy F_{el}, (From mechanical to microstructure) is added to total energy, and is calculated as

$$F_{el} = h(c) f_{el} \quad (12)$$

The variation of mechanical properties with respect to phase field variables are:

$$E(c) = (3c^2 - 2c^3) \cdot E_{particle} \quad (13)$$
$$\nu(c) = (3c^2 - 2c^3) \cdot \nu_{particle} \quad (14)$$

3) Thermo-mechanical coupling

Since the sintering process takes place at high temperatures, this leads to variation in the mechanical properties of the material, in addition to the induction of thermal stresses. On the other hand, the elastic energy generated during the mechanical transformations, in reverse, influences the thermal field. But for this study, the influence of elastic energy on the thermal field was neglected, as well as the thermal strain.

III. Numerical Approach

A. Implementation details

The fully implicit finite element approach and the Newton method are applied to solve the above coupled model, by using the software MOOSE. The backward Euler scheme with adaptive time stepping is applied. For more details, see [13], [24], [31], [36]. The domain considered is 70 µm x 70 µm, for 2D simulations. Circular particles (diameter equal to 30 µm) are embedded inside the simulation domain that has a minimum contact point at the initial step. The initial mesh discretization is uniformly refined with size of 0.5 µm to get at least four elements on the phase field interface, but adaptive mesh is also applied in order to reduce the error in the FE solution for phase field equations (see [13], [28]).

B. Initial and boundary conditions

For thermal field, the heat conduction equation was solved with constant temperatures for the initial and boundary conditions. While for Phase Field equations, Periodic boundary conditions was applied and initial conditions are:

$$c, \eta_i = \begin{cases} 1 & inside \\ 0 & outside \end{cases} \quad the\ particule$$

For mechanical load application, all the sides are restricted to move in respective normal direction, the bottom surface is constrained in the x and y directions.

C. Simulations parameters

Temperature, time, and furnace atmosphere are the significant parameters that influence the ultimate outcomes of sintering [37], the sintering temperature should be around 70–90 % of the metal's melting point [3]. In this study the simulations were performed for different temperatures and time.

The material properties (Stain Steel: 316L), used are presented in Table 1 and 2. The simulations parameters are converted into dimensionless numbers using appropriate scales using the length, time and energy scale, once all equations need similar orders for numerical convergence of the residual.

TABLE I.

Simulations parameters [38], [39]	
Parameter (unit)	***Value***
k *(W/(m.K))*	$9.248 + 1.571 \cdot 10^{-2}T$
ρ *(Kg/m³)*	$8084.2 - 4.2086 \cdot 10^{-1}T - 3.8942 \cdot 10^{-5}T^2$
c_p *(J/(kg.K)))*	$469.75 + 13.49 \cdot 10^{-2}T$
V_m *(cm³/mol)*	7.012
γ_s *(J/m²)*	2.41
γ_{GB} *(J/m²)*	1.06
D_{ov} *(cm²/s)*	2.0
D_{ob} *(cm²/s)*	0.127
D_{os} *(cm²/s)*	4.10^3
Q_v *(eV)*	2.6
Q_b *(eV)*	0.58
Q_s *(eV)*	2.21
Q_m *(eV)*	0.171
M_{GB_0}*(m⁴/J/s)*	$5.53.10^{-8}$

IV. RESULTS AND DISCUSSION

To validate the model, some tests were performed, starting with a basic model of the sintering process, solving initially the phase field (microstructural field) with different constant temperatures (1200 K, 1400 K and 1600 K), and after the thermal and mechanical field was incorporated.

The numerical solution allowed to understand the behavior of the microstructure considering the evolution of porosity and the conserved phase variables, and also its influence on the behavior of the evolution of the material's thermomechanical properties.

The important aspects that can be observed are associated with the transformation of the grains into a single element (Figure 1), which causes the reduction of porosity and increases the density, and in general improves the thermomechanical properties. The temporal and spatial evolutions of temperature must be uniformly distributed to ensure the full and simultaneous activation of all particles within the domain.

Figure 1 illustrates the morphological evolution of the sintering process, indicating the crystallographic arrangement of the particles, as well as the reduction of porosity.

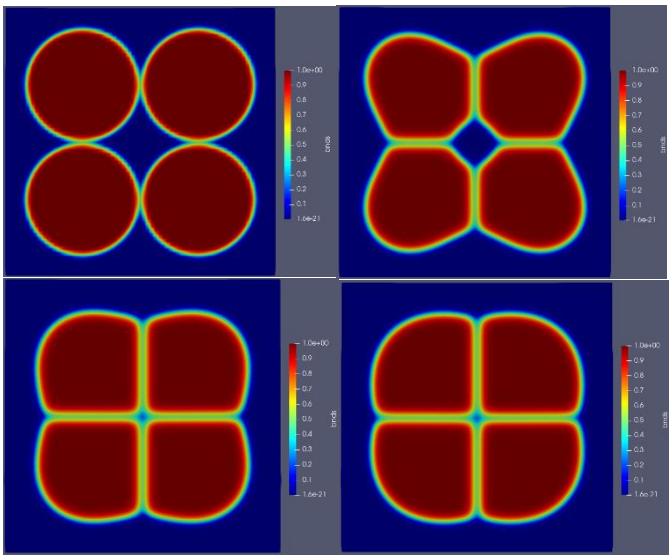

Figure 1: Microstructural evolution: non-conserved phase variable $\boldsymbol{\eta}$ (T = 1600 K) at simulated times (a) t = 0, (b) t = 5, (c) t = 10, (d) t = 30 s.

As expected, it was observed that for low temperature it requires a long time to achieve complete sintering, while high temperature leads to early sintering, as shown in figure 2 and 3. A stable sintering process needs a precise setting of temperature and time, and the simulation shows that the temperature of 1400 K, shows more stable results for almost all parameters and figure 4 indicates its numerical stability by the time step behavior.

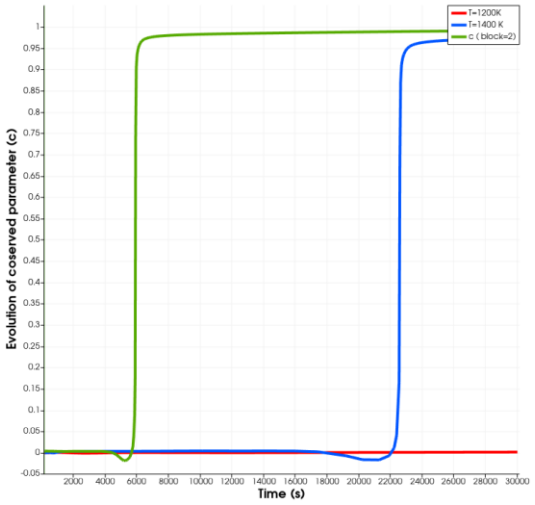

Figure 2: Evolution of conserved parameter c for 1200 K, 1400 K and 1600 K.

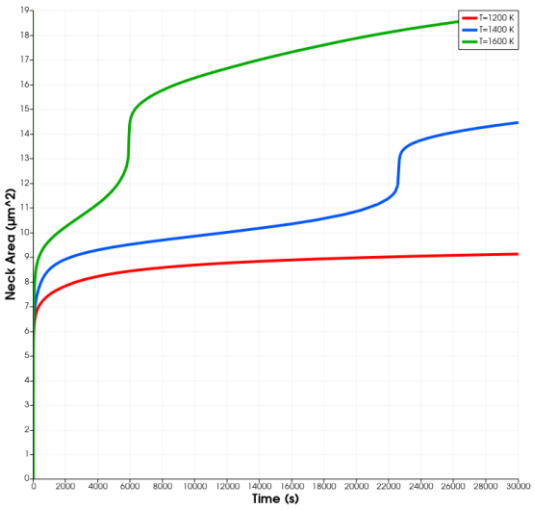

Figure 3: Evolution of neck area for 1200 K, 1400 K and 1600 K.

The neck area, which is formed by the bonding of the particles, can also be used to evaluate the porosity evolution. Figure 3 indicates that for the temperature of 1200 K and during the simulation time, the rate of this value is low, which implies that atomic diffusion is not sufficient for the particles to regroup and bond in order to eliminate all the voids between them.

Although diffusion is greater for high temperatures, however, it must occur in a controlled manner, under penalty of inducing large deformations in the component or structure during the

process, which reinforces the need to understand the effect of temperature.

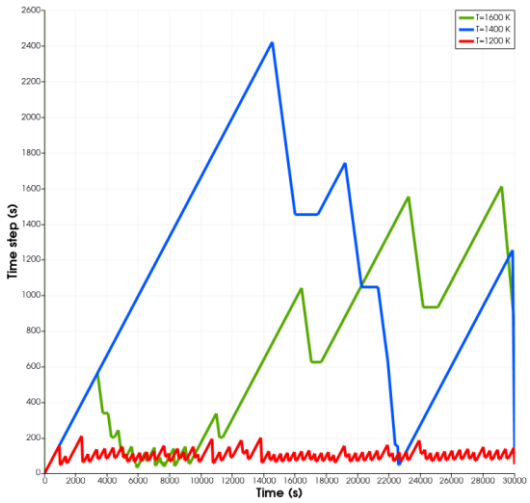

Figure 4: Behavior of the time step during the simulation, indicating the numerical stability of the model for different temperatures.

For solid-state sintering and pressure-less, the gravitational force becomes responsible for the mechanical deformations that occur in the component or structure during the process, however there is a relationship between temperature and the effect of gravity in the process, because of the density of the material that varies with temperature. Figure 5 shows that at higher temperatures greater shrinkage occurs, indicating greater deformation of the component or structure.

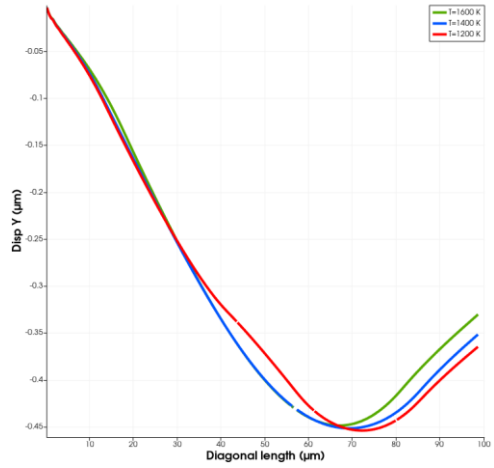

Figure 5: Distribution of the displacement in the y direction along the diagonal of the domain at the end of the simulation.

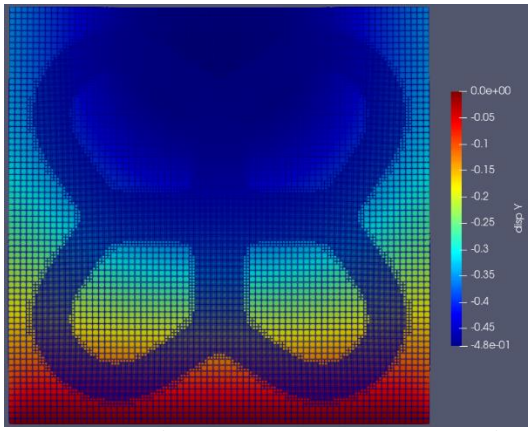

Figure 6: Distribution of the displacement in the y direction at final time.

It was observed that the distribution of the displacement in the y direction is symmetrical with respect to the domain under study, this is due to the behavior of gravity and the boundary conditions applied. As Figure 6 indicates, the closer to the base the smaller the shrinkage, while the largest shrinkages occur in areas near the top, which makes the effect of gravity as being one of the biggest problem in the application of sintering for complex components or structures.

V. Conclusion and Perspectives

A numerical model coupling multiphysics phenomena was presented to understand the behavior of the solid-state sintering process at microstructural level. The thermal field is the main driving force of the process, coupled with the gravity force as the main driving force of the mechanical field. The study also allowed to evaluate the effect of gravity on the microstructure evolution. The study allows the following conclusions and perspectives:

- The numerical coupling of the heat transfer, phase field equations and solids mechanic can be applied to predict the behavior of the solid state sintering process at microstructural level.
- The heat transfer leads to the activation of the microstructural field through the mechanisms of mass transport (diffusion process) and then the evolution of the phase field variables influences the thermomechanical properties of the material.
- The convergence of the thermal field is much faster than the microstructural and mechanical fields, so simulations at constant temperatures can be a good alternative to reduce computational time.
- The temperature selection must be after a thorough study of the material to be processed, as well as the

geometry of the component or structure, because of its impact on deformations.

- The introduction of the effect of gravity on the model makes the computational modeling of the solid-state sintering process more realistic.

ACKNOWLEDGMENT

The authors would like to extend a special note of thanks to Dr. Sudipta BISWAS for her advice. The authors thank TotalEnergies and France Embassy in Angola for the financial support.

REFERENCES

[1] S. Cooke, K. Ahmadi, S. Willerth, and R. Herring, "Metal additive manufacturing: Technology, metallurgy and modelling," *J. Manuf. Process.*, vol. 57, pp. 978–1003, Sep. 2020, doi: 10.1016/j.jmapro.2020.07.025.

[2] W. E. Frazier, "Metal Additive Manufacturing: A Review," *J. Mater. Eng. Perform.*, vol. 23, no. 6, pp. 1917–1928, Jun. 2014, doi: 10.1007/s11665-014-0958-z.

[3] M. Armstrong, H. Mehrabi, and N. Naveed, "An overview of modern metal additive manufacturing technology," *J. Manuf. Process.*, vol. 84, pp. 1001–1029, Dec. 2022, doi: 10.1016/j.jmapro.2022.10.060.

[4] H. E. Exner and E. Arzt, "CHAPTER 31 - SINTERING PROCESSES," in *Physical Metallurgy (Fourth Edition)*, R. W. Cahn and P. Haasen†, Eds. Oxford: North-Holland, 1996, pp. 2627–2662. doi: 10.1016/B978-044489875-3/50036-3.

[5] J. E. Blendell and W. Rheinheimer, "Solid-State Sintering," in *Encyclopedia of Materials: Technical Ceramics and Glasses*, M. Pomeroy, Ed. Oxford: Elsevier, 2021, pp. 249–257. doi: 10.1016/B978-0-12-803581-8.12084-3.

[6] R. German, "Sintering: From Empirical Observations to Scientific Principles," *Sinter. Empir. Obs. Sci. Princ.*, pp. 1–536, 2014, doi: 10.1016/C2012-0-00717-X.

[7] B. Dutta, S. Babu, and B. Jared, "Chapter 7 - Design for metal additive manufacturing," in *Science, Technology and Applications of Metals in Additive Manufacturing*, B. Dutta, S. Babu, and B. Jared, Eds. Elsevier, 2019, pp. 193–244. doi: 10.1016/B978-0-12-816634-5.00007-8.

[8] M. Kamal and G. Rizza, "4 - Design for metal additive manufacturing for aerospace applications," in *Additive Manufacturing for the Aerospace Industry*, F. Froes and R. Boyer, Eds. Elsevier, 2019, pp. 67–86. doi: 10.1016/B978-0-12-814062-8.00005-4.

[9] M. A. Mechter, Y. Mace, and O. Kerbrat, "A new design for additive manufacturing method: applied on the bound metal deposition process," *J. Eng. Des.*, vol. 33, no. 10, pp. 787–810, Oct. 2022, doi: 10.1080/09544828.2022.2136478.

[10] J. Gonzalez-Gutierrez, S. Cano, S. Schuschnigg, C. Kukla, J. Sapkota, and C. Holzer, "Additive Manufacturing of Metallic and Ceramic Components by the Material Extrusion of Highly-Filled Polymers: A Review and Future Perspectives," *Materials*, vol. 11, no. 5, Art. no. 5, May 2018, doi: 10.3390/ma11050840.

[11] C. Suwanpreecha and A. Manonukul, "A Review on Material Extrusion Additive Manufacturing of Metal and How It Compares with Metal Injection Moulding," *Metals*, vol. 12, no. 3, Art. no. 3, Mar. 2022, doi: 10.3390/met12030429.

[12] R. Shi, M. Wood, T. W. Heo, B. C. Wood, and J. Ye, "Towards understanding particle rigid-body motion during solid-state sintering," *J. Eur. Ceram. Soc.*, Sep. 2021, doi: 10.1016/j.jeurceramsoc.2021.09.039.

[13] S. Biswas, D. Schwen, and V. Tomar, "Implementation of a phase field model for simulating evolution of two powder particles representing microstructural changes during sintering," *J. Mater. Sci.*, vol. 53, no. 8, pp. 5799–5825, Apr. 2018, doi: 10.1007/s10853-017-1846-3.

[14] R. Bordia, S. Kang, and E. Olevsky, "Current understanding and future research directions at the onset of the next century of sintering science and technology," *J. Am. Ceram. Soc.*, vol. 100, Apr. 2017, doi: 10.1111/jace.14919.

[15] J. Merhar, "Overview of metal injection moulding," *Met. Powder Rep.*, vol. 45, no. 5, pp. 339–342, May 1990, doi: 10.1016/S0026-0657(10)80242-5.

[16] A. Molinari, "Fundamentals of Sintering: Solid State Sintering," in *Reference Module in Materials Science and Materials Engineering*, Elsevier, 2021. doi: 10.1016/B978-0-12-819726-4.00096-X.

[17] S. Kang, *Sintering: Densification, Grain Growth & Microstructure*. 2005.

[18] D. Vallauri and G. Maizza, "Simulation of Solid State Sintering through FE Modeling for the Optimum Design of 3D Parts," *Adv. Eng. Mater.*, vol. 6, no. 12, pp. 952–957, 2004, doi: https://doi.org/10.1002/adem.200400104.

[19] W. Niu and J. Pan, "Computer modelling of sintering: theory and examples," in *Sintering of Advanced Materials*, Z. Z. Fang, Ed. Woodhead Publishing, 2010, pp. 86–109. doi: 10.1533/9781845699949.1.86.

[20] M. Braginsky, V. Tikare, and E. Olevsky, "Numerical simulation of solid state sintering," *Int. J. Solids Struct.*, vol. 42, no. 2, pp. 621–636, Jan. 2005, doi: 10.1016/j.ijsolstr.2004.06.022.

[21] V. Tikare, M. Braginsky, D. Bouvard, and A. Vagnon, "Numerical simulation of microstructural evolution during sintering at the mesoscale in a 3D powder compact," *Comput. Mater. Sci.*, vol. 48, no. 2, pp. 317–325, Apr. 2010, doi: 10.1016/j.commatsci.2010.01.013.

[22] J. Hötzer, M. Seiz, M. Kellner, W. Rheinheimer, and B. Nestler, "Phase-field simulation of solid state sintering," *Acta Mater.*, vol. 164, pp. 184–195, Feb. 2019, doi: 10.1016/j.actamat.2018.10.021.

[23] Y. U. Wang, "Computer modeling and simulation of solid-state sintering: A phase field approach," *Acta Mater.*, vol. 54, no. 4, pp. 953–961, Feb. 2006, doi: 10.1016/j.actamat.2005.10.032.

[24] S. Biswas, D. Schwen, J. Singh, and V. Tomar, "A study of the evolution of microstructure and consolidation kinetics during sintering using a phase field modeling based approach," *Extreme Mech. Lett.*, vol. 7, pp. 78–89, Jun. 2016, doi: 10.1016/j.eml.2016.02.017.

[25] J.-Q. Li, T.-H. Fan, T. Taniguchi, and B. Zhang, "Phase-field modeling on laser melting of a metallic powder," *Int. J. Heat Mass Transf.*, vol. 117, pp. 412–424, Feb. 2018, doi: 10.1016/j.ijheatmasstransfer.2017.10.001.

[26] S. Biswas, D. Schwen, H. Wang, M. Okuniewski, and V. Tomar, "Phase field modeling of sintering: Role of grain orientation and anisotropic properties," *Comput. Mater. Sci.*, vol. 148, pp. 307–319, Jun. 2018, doi: 10.1016/j.commatsci.2018.02.057.

[27] R. Termuhlen, X. Chatzistavrou, J. D. Nicholas, and H.-C. Yu, "Three-dimensional phase field sintering simulations accounting for the rigid-body motion of individual grains," *Comput. Mater. Sci.*, vol. 186, p. 109963, Jan. 2021, doi: 10.1016/j.commatsci.2020.109963.

[28] K. Chockalingam, V. G. Kouznetsova, O. van der Sluis, and M. G. D. Geers, "2D Phase field modeling of sintering of silver nanoparticles," *Comput. Methods Appl. Mech. Eng.*, vol. 312, pp. 492–508, Dec. 2016, doi: 10.1016/j.cma.2016.07.002.

[29] N. Moelans, B. Blanpain, and P. Wollants, "An introduction to phase-field modeling of microstructure evolution," *Calphad*, vol. 32, no. 2, pp. 268–294, Jun. 2008, doi: 10.1016/j.calphad.2007.11.003.

[30] J. W. Cahn and J. E. Hilliard, "Free Energy of a Nonuniform System. I. Interfacial Free Energy," *J. Chem. Phys.*, vol. 28, no. 2, pp. 258–267, Feb. 1958, doi: 10.1063/1.1744102.

[31] V. Ivannikov, F. Thomsen, T. Ebel, and R. Willumeit-Römer, "Capturing shrinkage and neck growth with phase field simulations of the solid state sintering," *Model. Simul. Mater. Sci. Eng.*, vol. 29, no. 7, p. 075008, Sep. 2021, doi: 10.1088/1361-651X/ac1f87.
[32] A. G. Khachaturyan, *Theory of Structural Transformations in Solids*. Courier Corporation, 2013.
[33] S. Y. Hu and L. Q. Chen, "A phase-field model for evolving microstructures with strong elastic inhomogeneity," *Acta Mater.*, vol. 49, no. 11, pp. 1879–1890, Jun. 2001, doi: 10.1016/S1359-6454(01)00118-5.
[34] M. Tonks, P. Millett, W. Cai, and D. Wolf, "Analysis of the elastic strain energy driving force for grain boundary migration using phase field simulation," *Scr. Mater.*, vol. 63, no. 11, pp. 1049–1052, Nov. 2010, doi: 10.1016/j.scriptamat.2010.07.034.
[35] I. Steinbach, "Phase-field models in materials science," *Model. Simul. Mater. Sci. Eng.*, vol. 17, no. 7, p. 073001, Jul. 2009, doi: 10.1088/0965-0393/17/7/073001.
[36] C. J. Permann *et al.*, "MOOSE: Enabling massively parallel multiphysics simulation," *SoftwareX*, vol. 11, p. 100430, Jan. 2020, doi: 10.1016/j.softx.2020.100430.
[37] H. Ramazani and A. Kami, "Metal FDM, a new extrusion-based additive manufacturing technology for manufacturing of metallic parts: a review," *Prog. Addit. Manuf.*, vol. 7, no. 4, pp. 609–626, Aug. 2022, doi: 10.1007/s40964-021-00250-x.
[38] J. L. Straalsund and J. F. Bates, "Partial molar volumes and size factor data for alloy constituents of stainless steel," *Metall. Mater. Trans. B*, vol. 5, no. 2, pp. 493–498, Feb. 1974, doi: 10.1007/BF02644119.
[39] X. Zhang and Y. Liao, "A phase-field model for solid-state selective laser sintering of metallic materials," *Powder Technol.*, vol. 339, pp. 677–685, Nov. 2018, doi: 10.1016/j.powtec.2018.08.025.